Carrier Effect on the Nature of V^{4+} and Active Oxygen Species in Vapor-phase Oxidation of Butadiene over Supported Divanadium Pentaoxide Catalysts

Masamichi Akimoto,* Masahiro Usami, and Etsuro Echigoya
Department of Chemical Engineering, Tokyo Institute of Technology, Ookayama, Meguro-ku, Tokyo 152

(Received January 13, 1978)

The reactivity of V^{4+} with gaseous oxygen formed on various kinds of supported V_2O_5 catalysts has been investigated by ESR. The results are discussed as carrier effect in relation to the selectivity for maleic anhydride formation during the course of the vapor-phase oxidation of butadiene. V^{4+} formed on Al_2O_3 ($V/Al \leq 10/90$ atom ratio) and MgO ($V/Mg \leq 30/70$) showed a hyperfine ESR structure and was hardly oxidized whereas V^{4+} formed on SiO_2 ($V/Si \geq 5/95$) had the singlet ESR signal and was easily oxidized. Formation of these two kinds of V^{4+} was observed on V_2O_5–Al_2O_3 ($V/Al \geq 20/80$). They were similarly observed in the case of V_2O_5–TiO_2, but some portion of V^{4+} having the hyperfine structure was also oxidized. The selectivity was high over the catalysts forming the reactive V^{4+} as compared with those forming the unreactive one. The reactive V^{4+} was shown by X-ray diffraction to be preferentially formed in crystalline V_2O_5. Study of the reduction and reoxidation of unsupported crystalline V_2O_5 by means of IR and the effect of addition of alkali metal oxide on the catalytic activity of the supported V_2O_5 were discussed. The important role of double bond type lattice oxygen V=O in maleic anhydride formation was proposed.

In heterogeneous catalysis, a carrier is generally used for supporting the active component. However, the nature of the active site is strongly influenced by the kind of carrier, the supporting not always leading to better result. Thus, there are some observations which imply a chemical interaction between active component and carrier which may give rise to a carrier effect.[1–3] In heterogeneous oxidation of hydrocarbons, in which use of a carrier is strongly desirable, the role of carrier is not fully understood. In a previous paper,[4] a report was given on the carrier effect on the nature of supported molybdena catalyst in vapor-phase oxidation of butadiene. It was shown that the catalyst forming Mo^{5+} which is easily oxidized by gaseous oxygen has higher selectivity to maleic anhydride formation than that giving Mo^{5+} which is not oxidized. We have carried out a detailed investigation of carrier effect in the same catalytic oxidation using various supported V_2O_5 catalysts. Alumina, silica, titania, and magnesia were used as carrier, and the physical and chemical properties of these catalysts were investigated by X-ray analysis, ESR and IR spectroscopy in relation to the selectivity for maleic anhydride formation. Oxygen species, which is active and selective for the production of maleic anhydride, was also studied.

Experimental

The apparatus and procedure used for the oxidation were the same as those reported.[4] Pure butadiene (99.9% up) was used. Various supported V_2O_5 catalysts were prepared by mechanically kneading either alumina gel, silica gel, titania gel, or magnesium hydroxide with an aqueous solution of ammonium metavanadate for 3 h, evaporating the cake to dryness on a water bath and sieving the dried mass obtained into particles of 32—60 mesh. The catalysts were then calcined in an air current at 550 °C for 3 h. Titania gel was prepared by hydrolysis of titanium tetrachloride of reagent grade. Supported V_2O_5 catalysts modified with alkali metal oxide were prepared similarly. As a source of the metal oxide, extra pure alkali metal nitrates were used.

The gaseous effluent from the reactor was analyzed by gas chromatography. PEG 20M 20 wt% on Neopak 1A (60 °C, furan, acrylaldehyde, acetaldehyde), propylene carbonate 40 wt% on Celite 545 (room temp, butadiene, CO_2) and molecular sieve 13X (room temp, CO, N_2, O_2) were used as separating columns. Since maleic anhydride was the only acid obtained, the product was absorbed into water followed by titration with an aqueous solution of sodium hydroxide (0.1 M) after boiling off carbon dioxide. The structure of the catalysts was investigated by X-ray diffraction using nickel-filtered Cu $K\alpha$ radiation. The surface area of the catalysts was determined by the BET method using nitrogen as an adsorbate. A JEOL JES-PE-2X ESR spectrometer was used, in which microwave frequency was the X band and 100 kHz modulation was adopted. The amount of V^{4+} was measured using Mn^{2+} and DPPH as an internal standard. A Hitachi EPI-G3 spectrometer was used for IR studies.

Results

The Oxidation of Butadiene over Various Supported V_2O_5 Catalysts. Alumina, silica, titania, and magnesia showed negligible activity in the oxidation of butadiene. The carriers promoted only complete combustion of butadiene without formation of maleic anhydride. Figure 1 shows the result of oxidation over V_2O_5–Al_2O_3 catalyst. The catalyst containing V_2O_5 at $V/Al=5/95$ atom ratio had a negligible activity. However, further addition of V_2O_5 enhanced the activity to reach a maximum value at $V/Al=20/80$. The selectivity to maleic anhydride was low, *i.e.*, 6.5% over the catalyst of $V/Al=10/90$ in contrast to those (30—35%) over the catalysts of $V/Al \geq 20/80$.

The catalytic activity of V_2O_5–SiO_2 increased with increase in the content of V_2O_5 (Fig. 2). V_2O_5–TiO_2 showed a tendency similar to that of V_2O_5–Al_2O_3 (Fig. 3). However, in contrast to the latter catalyst, the former two catalysts had an ability of producing maleic anhydride in spite of the low content of V_2O_5, *i.e.*, $V/Si=5/95$ and $V/Ti=5/95$. V_2O_5–MgO ($V/Mg \leq 30/70$) formed no maleic anhydride; conversion of butadiene and yield of CO_2 and CO were 24.9, 24.2% ($V/Mg=5/95$), 39.6, 33.7% (10/90), 58.9, 55.4%

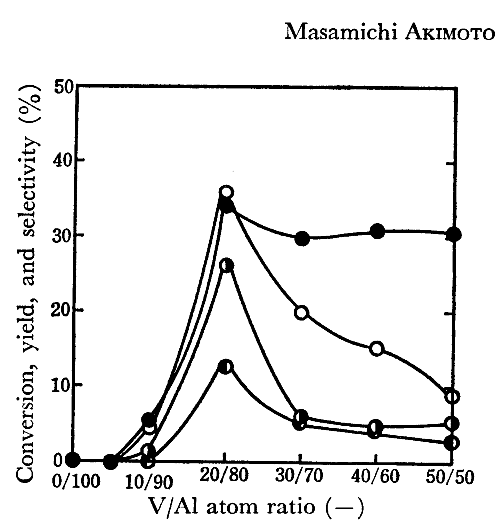

Fig. 1. The oxidation of butadiene over various V_2O_5–Al_2O_3 catalysts. Reaction temp (bath): 310 °C, feed: butadiene 1.45 vol% in air, contact time: $W/F=0.373$ g-cat·h/g-mol.

○: Conversion of butadiene, ◑: yield of CO_2+CO, ◐: yield of maleic anhydride, ●: selectivity to maleic anhydride.

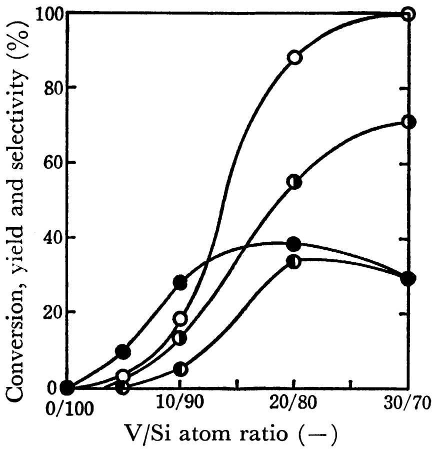

Fig. 2. The oxidation of butadiene over various V_2O_5–SiO_2 catalysts. Reaction temp (bath): 380 °C, feed: butadiene 1.45 vol% in air, contact time: $W/F=0.373$ g-cat·h/g-mol. Symbols are the same as those in Fig. 1.

(20/80), and 57.0, 57.4% (30/70), respectively, at 425 °C, contact time $W/F=1.490$ g-cat·h/g-mol and butadiene 1.45 vol% in air.

Based on the selectivity to maleic anhydride formation, these catalysts can be divided into the following three groups;

(A) V_2O_5–Al_2O_3 (V/Al=5/95 and 10/90), V_2O_5–MgO (V/Mg≤30/70).

The selectivity is negligible or very low.

(B) V_2O_5–SiO_2 (V/Si=5/95), V_2O_5–TiO_2 (V/Ti=5/95).

The selectivity is 10—16%.

(C) V_2O_5–Al_2O_3 (V/Al≥20/80), V_2O_5–SiO_2 (V/Si≥10/90), and V_2O_5–TiO_2 (V/Ti≥10/90).

The selectivity is 30—39%.

X-Ray Studies on the Supported V_2O_5 Catalysts. Al_2O_3 and SiO_2 were almost amorphous, the former showing weak X-ray diffraction at $2\theta=46.0$ and 67.0°. Thus, Al_2O_3 was γ-type. In the case of V_2O_5–Al_2O_3, the diffraction due to crystalline V_2O_5 appeared from

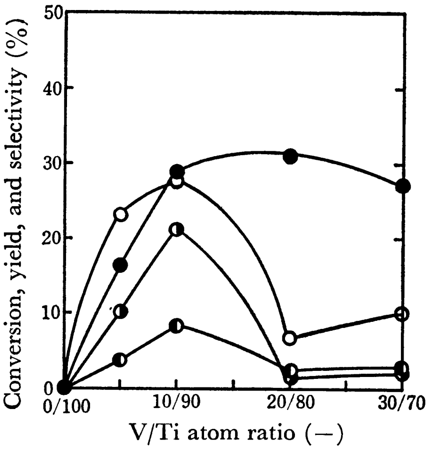

Fig. 3. The oxidation of butadiene over various V_2O_5–TiO_2 catalysts. Reaction temp (bath): 300°C, feed: butadiene 1.32 vol%, oxygen 9.11 vol%, diluent–nitrogen, contact time: $W/F=0.325$ g-cat·h/g-mol. Symbols are the same as those in Fig. 1.

V/Al=20/80 ($2\theta=25.6°$), its strength increasing with rise in the content of V_2O_5; *i.e.*, V_2O_5–Al_2O_3 (V/Al=40/60) showed diffraction at $2\theta=20.5$, 26.1, 31.0° (strong), 15.5, 21.8, 32.4, and 34.4° (medium). On the other hand, the presence of crystalline V_2O_5 was observed from V/Si=10/90 ($2\theta=15.4$, 26.0, and 32.2°), its amount increasing with rise in content. TiO_2 was of anatase-type ($2\theta=25.2$, 37.9, 48.0, and 54.0°), formation of the V_2O_5 being distinctly observed at V/Ti≥20/80 ($2\theta=15.2$, 20.2, 26.2, and 31.3°). In contrast, V_2O_5–MgO (V/Mg≤30/70) showed strong X-ray diffraction due to periclase-type MgO at $2\theta=36.9$, 42.7, and 62.1° with a very weak diffraction due to V_2O_5 at $2\theta=35.1°$ (V/Mg≥10/90). Thus, the group C catalysts contain crystalline V_2O_5 in contrast to groups A and B.

ESR Spectrum of V^{4+} and Its Reactivity to Gaseous Oxygen. Formation of paramagnetic species in various V_2O_5 catalysts preevacuated at 450 °C under 10^{-5} mmHg was investigated by means of ESR. V_2O_5–SiO_2 (V/Si=5/95) gave a singlet spectrum, its *g*-factor being 1.98 and the linewidth expressed by maximum slope separation 107G. The line shape was nearly Lorentzian. This spectrum agreed with that of V^{4+} which forms a cluster in pure V_2O_5 and on Alundum carrier.[5] However, the linewidth increased with further rise in the content of V_2O_5 (V/Si=20/80, $\Delta H_{msl}=213$G).

A completely different spectrum was observed for V_2O_5–Al_2O_3 (V/Al≤10/90), V_2O_5–TiO_2 (V/Ti=5/95), and V_2O_5–MgO (V/Mg≤30/70), which clearly showed hyperfine splitting caused by the nuclear magnetic moment of vanadium $I=7/2$ (Fig. 4, V/Al=5/95). V_2O_5–Al_2O_3 (V/Al≥20/80) and V_2O_5–TiO_2 (V/Ti≥10/90) gave ESR spectra consisting of hyperfine structure and singlet. Analysis of the complicated spectrum having the hyperfine structure was carried out by the method developed by Hecht and Johnstone.[6] The spectrum was analyzed with an axial symmetric spin Hamiltonian[7]

$$\mathscr{H} = \beta(g_{\parallel}H_zS_z + g_{\perp}H_xS_x + g_{\perp}H_yS_y) + A_{\parallel}S_zI_z + A_{\perp}S_xI_x + A_{\perp}S_yI_y, \quad (1)$$

where β is the Bohr magneton, $g_{\parallel}$ and $g_{\perp}$ are the parallel and perpendicular principal components, respectively, of the g-tensor; $A_{\parallel}$ and $A_{\perp}$ are the parallel and perpendicular principal components, respectively, of the hyperfine-coupling tensor; H_x, H_y, H_z are the components of the magnetic field; S_x, S_y, S_z, and I_x, I_y, I_z are the components of spin operators of the electron and nucleus, respectively, the coordinate system being fixed to the molecule. The absorption peaks are related to $2I+1$ values of m_I, the peaks appearing in the field of

$$H_{\parallel} = 2H_0/g_{\parallel} - (A_{\parallel}/g_{\parallel}\beta)m_I \quad (\text{for } \theta = 0), \qquad (2)$$

$$H_{\perp} = 2H_0/g_{\perp} - (A_{\perp}/g_{\perp}\beta)m_I \quad (\text{for } \theta = \pi/2), \qquad (3)$$

where θ is the angle spanning between H_0 and the axial symmetry axis of the ion site. Plotting the magnetic field of the observed peaks corresponding to either $H_{\parallel}$ or $H_{\perp}$ against the nuclear quantum number m_I, we obtain a linear relation. The slopes and the intercepts with the $m_I=0$ line can be used to obtain values of the parameters, $g_{\parallel}$, $A_{\parallel}$, $g_{\perp}$, and $A_{\perp}$. Assignment of the peaks of the observed spectrum was attained according to the method used by Takahashi *et al.*[5] The result is illustrated as two sets of octets as shown in Fig. 4 (V/Al=5/95). The values of the parameters are given in Table 1. The observed components of the g-factor show that the g-tensor of V^{4+} ion has axial symmetry. The observed parameters agree with those of the V^{4+} formed separately on Neobead carrier.[5]

Reactivity of V^{4+} with gaseous oxygen was investigated by introduction of 20 mmHg O_2 followed by heating at various temperatures for 30 min. The amount of V^{4+} existing after the reaction was determined at room temperature. V^{4+} in V_2O_5–Al_2O_3 (V/Al≤10/90) was scarcely oxidized even at 450 °C, but a large portion of V^{4+} in V_2O_5–Al_2O_3 (V/Al≥20/80) was oxidized to V^{5+} above 200 °C with simultaneous appearance of the hyperfine structure. V^{4+} in V_2O_5–MgO (V/Mg≤30/70) was also hardly oxidized at 450 °C whereas that in V_2O_5–SiO_2 (V/Si≤30/70) was easily oxidized. Thus, V^{4+} having the singlet spectrum is reactive to oxygen, but not the one having hyperfine structure. However, some portion of V^{4+} formed in V_2O_5–TiO_2 (V/Ti=5/95) was easily oxidized irrespective of the hyperfine structure. V^{4+} in V_2O_5–TiO_2 (V/Ti≥10/90) showed a reactivity similar to that in V_2O_5–Al_2O_3 (V/Al≥20/80). The observations are summarized in Table 2. The catalysts forming reactive V^{4+} have high selectivity as compared with those having unreactive V^{4+}. The reactive V^{4+} is preferentially formed in crystalline V_2O_5.

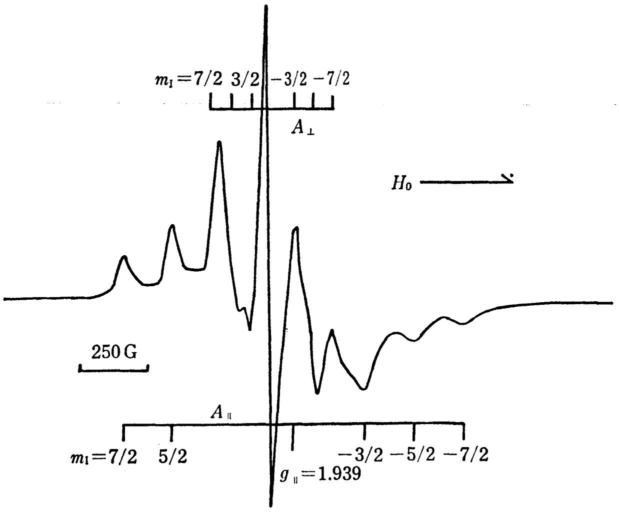

Fig. 4. ESR spectrum of V^{4+} formed in V_2O_5–Al_2O_3(V/Al=5/95). Catalyst: evacuated at 450 °C and 10^{-5} mmHg for 2 h. ESR: measured at room temperature.

Correlation Existing between the Amount of V^{4+} and the Catalytic Activity. The amount of V^{4+} formed by the evacuation of various V_2O_5–Al_2O_3 at 450 °C and decreased on contact with gaseous oxygen at 350 °C were determined (Table 3). 0.4—1.2% of vanadium present in the catalyst is V^{4+}, in line with the other catalysts. The amount of V^{4+} which is reactive to

Table 1. Spin Hamiltonian parameters of the spectrum of V^{4+} on various carriers

Catalyst(atom ratio)	$\lvert A_{\parallel}\rvert$	$\lvert A_{\perp}\rvert$	$\lvert A_0\rvert$	$g_{\parallel}$	$g_{\perp}$	g_0	$H_{\parallel}(m_I=0)$	$H_{\perp}(m_I=0)$
V_2O_5–Al_2O_3 (V/Al=5/95)	161×10^{-4} cm^{-1} 178G	56×10^{-4} cm^{-1} 61G	91×10^{-4} cm^{-1} 100G	1.939	1.983	1.968	3399G	3324G
V_2O_5–Al_2O_3 (V/Al=10/90)	161×10^{-4} cm^{-1} 177G	57×10^{-4} cm^{-1} 62G	92×10^{-4} cm^{-1} 100G	1.944	1.976	1.965	3383G	3328G
V_2O_5–TiO_2 (V/Ti=5/95)	167×10^{-4} cm^{-1} 180G	56×10^{-4} cm^{-1} 61G	93×10^{-4} cm^{-1} 101G	1.922	1.983	1.963	3427G	3324G
V_2O_5–MgO (V/Mg=20/80)	160×10^{-4} cm^{-1} 177G	59×10^{-4} cm^{-1} 64G	93×10^{-4} cm^{-1} 102G	1.936	1.976	1.963	3408G	3339G

$\lvert A_0\rvert$, g_0: calculated values.

Table 2. Summary of the characteristics of various supported V_2O_5 catalysts

Catalyst group	Selectivity to MA (%)	Presence of crystalline V_2O_5	Nature of V^{4+}	
			ESR spectrum	Reactivity to O_2
A	≈0	no	h.f.s.	no
B	10—16	no	singlet (V/Si=5/95) h.f.s. (V/Ti=5/95)	yes
C	30—39	yes	singlet (V/Si≥10/90) singlet+h.f.s. (V/Al, V/Ti≥20/80)	no (h.f.s.) yes (singlet)

Table 3. The amount of V^{4+} formed in V_2O_5–Al_2O_3 catalysts

V/Al atom ratio(—)	Surface area (m^2/g)	V^{4+}formed (spins/g-cat)[a]	V^{4+}/total V(%)	Reactive V^{4+} [b]
0/100	—	0.00	—	0.00
5/95	338	0.71×10^{19}	1.27	neg.
10/90	353	0.67×10^{19}	0.61	neg.
20/80	77	1.55×10^{19}	0.69	0.61×10^{19}
30/70	68	1.15×10^{19}	0.40	0.35×10^{19}
40/60	59	1.42×10^{19}	0.39	0.34×10^{19}
50/50	66	2.80×10^{19}	0.66	0.31×10^{19}

a) Evacuated at 450 °C and 10^{-5} mmHg for 2 h. b) The amount of V^{4+} (spins/g-cat.) decreased on contact with gaseous oxygen (20 mmHg) at 350 °C for 30 min.

oxygen increased suddenly with increase in the content of V_2O_5, reaching a maximum value at V/Al=20/80, decreasing gradually with further increase. The amount is not that of reactive V^{4+} existing on the surface. However, increase in the yield of maleic anhydride with increase in amount also indicates the important role of the reactive V^{4+} in the anhydride formation.

IR Studies on the Reduction and Reoxidation of V_2O_5. The above results reveal that the reactive V^{4+} formed in crystalline V_2O_5 is important for anhydride formation. In order to clarify the kind of lattice oxygen participating in the reduction-oxidation of V_2O_5, unsupported crystalline V_2O_5 was used in IR studies instead of the group C catalysts. Absorption bands were obtained at about 1020 cm^{-1} ($\nu_{V^{5+}=O}$) and 830 cm^{-1} (ν_{V-O-V}).[8–10] Effect of the reduction of this V_2O_5 with a current of hydrogen at 512 °C on the ratio of the peak area of these absorption bands was investigated. Gradual decrease in the ratio with rise in the reduction time was observed, a small lower shift of these bands taking place (Table 4). Formation of V^{4+}=O or VO_2 was confirmed by the appearance of a new absorption band at 980 cm^{-1},[8,11] its intensity increasing with increase in reduction time. The results are the same as those reported.[12,13] The original absorption bands were easily recovered by the reoxidation of the reduced V_2O_5 with a current of air at the same temperature. Thus, double bond type lattice oxygen V^{5+}=O in crystalline V_2O_5 is first reduced to give reactive V^{4+} and is recovered by reoxidation.

Table 4. Change in the ratio of IR absorption peak area ($\nu_{V^{5+}=O}/\nu_{V-O-V}$) with the reduction of unsupported V_2O_5[a]

Reduction time/min	$\nu_{V^{5+}=O}$/cm^{-1}	ν_{V-O-V}/cm^{-1}	Ratio of the peak area ($\nu_{V^{5+}=O}/\nu_{V-O-V}$)
0	1017	830	—
5	1014	820	0.473
10	1008	825	0.454
15	1005	825	0.403

a) KBr disk technique: Reduction temp: 512 °C, V_2O_5: 0.5 g, Flow rate of hydrogen: *ca.* 50 NTPml/min.

Effect of the Addition of Alkali Metal Oxide on the Catalytic Activity of Supported V_2O_5 Catalysts. The effect of addition of alkali metal oxide on the formation of maleic anhydride was studied using V_2O_5–Al_2O_3 (V/Al=20/80) and V_2O_5–SiO_2 (V/Si=20/80). The rate of maleic anhydride formation per unit surface area measured by means of a differential reactor was enhanced with a decrease in the electronegativity of the metal ion added (Table 5).

Table 5. Effect of the addition of alkali metal oxide on the catalytic activity of supported V_2O_5 in the oxidation of butadiene

Alkali metal oxide	Electronegativity of alkali metal element[a]	Rate of maleic anhydride formation (g-mol/m^2-cat·h) V_2O_5–Al_2O_3 (V/Al=20/80)[b]	V_2O_5–SiO_2 (V/Si=20/80)[c]
Cs_2O	0.7	5.88×10^{-5}	5.20×10^{-5}
Rb_2O	0.8	3.81×10^{-5}	4.89×10^{-5}
K_2O	0.8	4.89×10^{-5}	4.61×10^{-5}
Na_2O	0.9	3.36×10^{-5}	4.26×10^{-5}
Li_2O	1.0	1.92×10^{-5}	3.98×10^{-5}

a) Pauling. b) Cat.: V/Al=20/80 atom ratio, alkali metal/V=1/100 atom ratio, Reaction temp: 315 °C, Feed: butadiene 1.45 vol% in air. c) Cat.: V/Si=20/80 atom ratio, alkali metal/V=0.5/100 atom ratio, Reaction temp: 340 °C, Feed: butadiene 1.45 vol% in air.

Discussion

The change in catalytic activity of V_2O_5–Al_2O_3 can be attributed not to that in the surface area but to the formation of active species by the addition of V_2O_5 to Al_2O_3 (Table 3). The active species is V^{4+}, which is the case in the other catalysts. However, the results obtained indicate that the nature of V^{4+} formed has strong effect on the selectivity to maleic anhydride formation. The catalysts having reactive V^{4+} had high selectivity to the anhydride, this kind of V^{4+} being formed preferentially in the crystalline V_2O_5 (Tables 2 and 3).

During the catalytic oxidation, V^{5+}=O in the crystalline V_2O_5 is first reduced to give V^{3+} as shown by IR studies (Table 4). The V^{3+} then forms V^{4+} and V^{4+}=O by donation of its one electron to a neighbouring V^{5+}=O, *i.e.*, $V^{3+}+V^{5+}\text{=O}\rightarrow V^{4+}+V^{4+}\text{=O}$. The V^{4+}=O is further reduced or recovered into original V^{5+}=O when V^{4+} is oxidized to V^{5+}=O. On the reactive V^{4+}, various electronegative oxygen species such as O_2^- and O^- are formed when gaseous oxygen is adsorbed.[14] At elevated temperature, these oxygen species change rapidly to lattice oxygen O^{2-}, instead V^{4+} being oxidized to V^{5+}. The lattice oxygen formed is of double bond type as shown by IR studies on the reoxidation of reduced V_2O_5. The high selectivity of V_2O_5 catalysts forming the reactive V^{4+} strongly suggests a very important role of the negatively charged oxygen species formed by the oxidation of V^{4+}. The reactive V^{4+} plays a role of a precursor which forms the oxygen species.

Generally, the strength of metal-oxygen bond increases in proportion to the electronegativity of metal ion.[15,16] Thus the reactivity of lattice oxygen decreases with rise in the electronegativity of metal ion. In contrast, the amount of oxygen species adsorbed increases with rise in electronegativity, rate of catalytic oxidation increasing when oxygen species adsorbed is important. This was confirmed by the oxidation of various hydrocarbons over MoO_3,17) TiO_2,18) and $Bi_2O_3$19) catalysts modified with oxide of 5B group element or of alkali metal. The electronegativity of these metal ion was shown to have changed in proportion to that of the metal ion added. On the analogy of the rsults, it can be expected that the electronegativity of vanadium ion modified with alkali metal oxide is $Li^+ > Na^+ > K^+ > Rb^+ > Cs^+$ as a sequence of alkali metal ion added, the reactivity of its lattice oxygen being $Cs^+ > Rb^+ > K^+ > Na^+ > Li^+$. Thus, increase in the rate of maleic anhydride formation with decrease in the electronegativity of alkali metal ion (Table 5) strongly supports participation of lattice oxygen rather than the adsorbed oxygen species in maleic anhydride formation over these catalysts. This lattice oxygen is considered to be of double bond type V=O as shown by IR studies. This is in line with the important role of Mo=O in the oxidation of butadiene to maleic anhydride over MoO_3 catalyst4) and with the special activity of the double bond type lattice oxygen proposed.10,20–22)

Lattice oxygen of transition metal oxide serves to abstract hydrogen irrespective of the type of metal-oxygen bonding (σ- and double bond one).20,23) However, the former lattice oxygen is not always incorporated into selective oxidation product.23) Maleic anhydride is formed from butadiene by the repetition of oxygen addition and hydrogen abstraction.24,25) Thus, it was considered that V=O is requisite as oxygen species incorporated into the anhydride. Possibly, this lattice oxygen also plays a role of hydrogen abstraction from intermediates leading to maleic anhydride. The oxygen species participating in the complete oxidation over the group A catalysts was not clarified. However, it is apparent that the electronegative oxygen species were hardly formed during the course of catalytic oxidation, as suggested by the unreactivity of V^{4+} to oxygen. Oxygen species participating in maleic anhydride formation over V_2O_5–SiO_2 (V/Si=5/95) seems to be the same as that over the group C catalysts as judged from the similarity in the ESR spectrum of V^{4+}. Those over V_2O_5–TiO_2 (V/Ti=5/95) were not clarified.

Structures of the catalysts are discussed. V^{4+} formed in a cluster has a singlet ESR spectrum and that formed separately a hyperfine structure, the distance between the nearest neighbour V^{4+} being <5 Å in the former V^{4+} and ≈ 9 Å in the latter.5) Vanadium ions in V_2O_5–MgO ($V/Mg \leq 30/70$) are finely dispersed in the carrier whereas V_2O_5 on SiO_2 ($V/Si \geq 5/95$) forms cluster. In the case of V_2O_5–Al_2O_3 and V_2O_5–TiO_2, vanadium ions are finely dispersed when the content of V_2O_5 is low ($V/Al \leq 10/90$, $V/Ti \leq 5/95$). Formation of V_2O_5 cluster takes place with increase in the content, thus giving the spectra made by overlap of these two kinds of ESR spectra. This explanation is in line with the observation of crystalline V_2O_5 by X-ray studies. V^{4+}, which is not oxidized with oxygen, is possibly formed from finely dispersed vanadium ions by a solid-phase reaction when the catalysts were prepared. V^{4+}, on the other hand, formed at the sites where lattice oxygen in V_2O_5 cluster is lost by evacuation, appears to be easily oxidized. The reactive nature of V^{4+} formed in V_2O_5–TiO_2 (V/Ti=5/95) to oxygen irrespective of the hyperfine structure is presumably attributed to a relatively large mobility of lattice oxygen in the titania as compared with the other carriers.

References

1) I. J. Adadurov, *J. Phys. Chem., USSR*, **6**, 206 (1935).

2) P. W. Selwood, "Advances in Catalysis," Vol. 3, Academic Press, New York (1951), p. 28.

3) F. Solymosi, "Catalysis Reviews," Vol. 1, Marcel Dekker Inc., New York (1968), p. 233.

4) M. Akimoto and E. Echigoya, *J. Catal.*, **29**, 191 (1973).

5) H. Takahashi, M. Shiotani, H. Kobayashi, and J. Sohma, *J. Catal.*, **14**, 134 (1969).

6) H. G. Hecht and T. S. Johnstone, *J. Chem. Phys.*, **46**, 23 (1967).

7) B. Bleaney, *Phil. Mag.*, **42**, 441 (1951).

8) L. D. Frederickson and D. M. Hansen, *Anal. Chem.*, **35**, 818 (1963).

9) B. E. Zeitsev and I. I. Ioffe, *Kinet. Katal.*, **7**, 755 (1966).

10) Y. Kera and K. Hirota, *J. Phys. Chem.*, **73**, 3973 (1969).

11) M. E. Brown and B. V. Sewart, *J. Thermal. Anal.*, **2**, 287 (1970).

12) S. Hasegawa, N. Miyazawa, S. Kitamori, and T. Kawaguchi, *Nippon Kagaku Kaishi*, **1975**, 246.

13) A. Miyamoto, Y. Yamazaki, and Y. Murakami, *Nippon Kagaku Kaishi*, **1977**, 619 (1977).

14) V. A. Shvets and V. B. Kazansky, *Kinet. Katal.*, **10**, 356 (1969): *J. Catal.*, **25**, 123 (1972).

15) A. F. Clifford, *J. Am. Chem. Soc.*, **79**, 5404 (1957); *J. Phys. Chem.*, **63**, 1227 (1959).

16) Y. Moro-oka, Y. Morikawa, and A. Ozaki, *J. Catal.*, **7**, 23 (1967).

17) M. Akimoto and E. Echigoya, *J. Catal.*, **35**, 278 (1974).

18) M. Akimoto and E. Echigoya, *J. Chem. Soc., Faraday Trans. 1*, **73**, 193 (1977).

19) M. Akimoto, K. Ichikawa, and E. Echigoya, *Nippon Kagaku Kaishi*, **1977**, 320.

20) F. Trifiro and I. Pasquon, *J. Catal.*, **12**, 412 (1968).

21) K. Tarama, S. Teranishi, and S. Yoshida, Proc. 3rd Int. Congr. Catal., Vol. 1, 3rd ed, North-Holland, Amsterdam (1964), p. 282.

22) K. Hirota, Y. Kera, and S. Teratani, *J. Phys. Chem.*, **72**, 3133 (1968).

23) T. Seiyama, M. Egashira, T. Sakamoto, and I. Aso, *J. Catal.*, **24**, 76 (1972); H. E. Swift, J. E. Bozik, and J. A. Ondrey, *J. Catal.*, **21**, 212 (1971) *etc.*

24) M. Ai, K. Harada, and S. Suzuki, *Kogyo Kagaku Zasshi*, **73**, 524 (1970).

25) M. Akimoto and E. Echigoya, *Bull. Chem. Soc. Jpn.*, **48**, 3518 (1975).